

## Publication VII

J. P. Pekola, V. F. Maisi, S. Kafanov, N. Chekurov, A. Kemppinen, Yu. A. Pashkin, O.-P. Saira, M. Möttönen, and J. S. Tsai. 2010. Environment-assisted tunneling as an origin of the Dynes density of states. *Physical Review Letters*, volume 105, number 2, 026803, 4 pages.

© 2010 American Physical Society (APS)

Reprinted by permission of American Physical Society.

## Environment-Assisted Tunneling as an Origin of the Dynes Density of States

J. P. Pekola,<sup>1</sup> V. F. Maisi,<sup>2</sup> S. Kafanov,<sup>1</sup> N. Chekurov,<sup>3</sup> A. Kemppinen,<sup>2</sup> Yu. A. Pashkin,<sup>4,\*</sup> O.-P. Saira,<sup>1</sup>  
M. Möttönen,<sup>1,5</sup> and J. S. Tsai<sup>4</sup>

<sup>1</sup>Low Temperature Laboratory, Aalto University, P.O. Box 13500, FI-00076 Aalto, Finland

<sup>2</sup>Centre for Metrology and Accreditation (MIKES), P.O. Box 9, 02151 Espoo, Finland

<sup>3</sup>Department of Micro and Nanosciences, Aalto University, P.O. Box 13500, FI-00076 Aalto, Finland

<sup>4</sup>NEC Nano Electronics Research Laboratories and RIKEN Advanced Science Institute,  
34 Miyukigaoka, Tsukuba, Ibaraki 305-8501, Japan

<sup>5</sup>Department of Applied Physics/COMP, Aalto University, P.O. Box 15100, FI-00076 Aalto, Finland

(Received 26 February 2010; published 6 July 2010)

We show that the effect of a high-temperature environment in current transport through a normal metal–insulator–superconductor tunnel junction can be described by an effective density of states in the superconductor. In the limit of a resistive low-Ohmic environment, this density of states reduces into the well-known Dynes form. Our theoretical result is supported by experiments in engineered environments. We apply our findings to improve the performance of a single-electron turnstile, a potential candidate for a metrological current source.

DOI: 10.1103/PhysRevLett.105.026803

PACS numbers: 73.40.Gk, 06.20.Jr, 72.70.+m, 73.20.At

**Introduction.**—The density of states (DOS) of the carriers governs the transport rates in a mesoscopic conductor [1], e.g., in a tunnel junction. Understanding the current transport in a junction in detail is of fundamental interest, but it plays a central role also in practical applications, for instance, in the performance of superconducting qubits [2], of electronic coolers and thermometers [3], and of a single-electron turnstile to be discussed in this Letter [4]. When one or both of the contacts of a junction are superconducting, the one-electron rates at small energy bias should vanish at low temperatures because of the gap in the Bardeen-Cooper-Schrieffer (BCS) DOS [5]. Yet, a small linear in voltage leakage current persists in the experiments [3,6–10] that can often be attributed to the Dynes DOS, a BCS-like expression with lifetime broadening [11,12]. A junction between two leads admits carriers to pass at a rate that depends on the DOS of the conductors, the occupation of the energy levels, and the number of conduction channels in the junction [13]. In general, basic one-electron tunneling coexists with many-electron tunneling, for instance, cotunneling in multijunction systems [14], or Andreev reflection in superconductors [15,16]. However, when the junction is made sufficiently opaque, a common situation in practice, only one-electron tunneling governed by the Fermi golden rule should persist. We demonstrate experimentally that the subgap current in a high-quality opaque tunnel junction between a normal metal and a superconductor can be ascribed to photon-assisted tunneling. We show theoretically that this leads exactly to the Dynes DOS with an inverse lifetime of  $e^2 k_B T_{\text{env}} R / \hbar^2$ , where  $T_{\text{env}}$  and  $R$  are the temperature and effective resistance of the environment.

We employ a tunnel junction with a normal metal–insulator–superconductor (NIS) structure; see Fig. 1(a). The essentially constant DOS in the normal metal renders

the NIS junction an ideal probe for the superconductor DOS. Because of the BCS energy gap in an NIS system, the tunneling current is expected to be exponentially suppressed with decreasing temperature. Yet in the experiments a small subgap current persists as shown in Fig. 1(b). This leakage is typically attributed to Andreev current [17–20], smeared DOS of the superconductor [21], nonvanishing DOS in the insulator within the gap [9], nonequilibrium quasiparticles [22], or physical imperfections in the junction. Our junctions, like the one in Fig. 1, are made opaque with large normal-state resistance  $R_T$  to efficiently suppress the Andreev current. A convenient way to account for the smearing of the  $IV$  characteristics is to use the so-called Dynes model [11,12] based on an expression of the BCS DOS with lifetime broadening. The Dynes DOS, normalized by the corresponding normal-state DOS, is given by

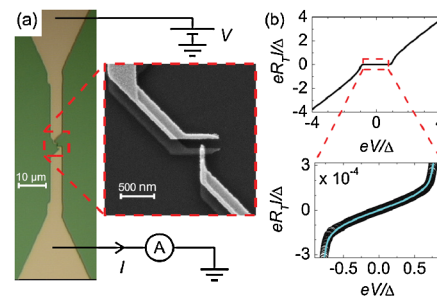


FIG. 1 (color online). (a) Geometry of the measured single NIS junctions made of aluminum (low contrast) as the superconductor and copper (high contrast) as the normal metal. The tapered ends lead to  $250 \times 250 \mu\text{m}^2$  pads. (b) Typical  $IV$  characteristics, measured at 50 mK for a sample with  $R_T = 30 \text{ k}\Omega$ . Linear leakage is observed deep in the gap region  $|eV| \ll \Delta \approx 200 \mu\text{eV}$ , consistent with the Dynes model using  $\gamma = 1.8 \times 10^{-4}$ , shown by the cyan line.

$$n_S^D(E) = \left| \Re e \left( \frac{E/\Delta + i\gamma}{\sqrt{(E/\Delta + i\gamma)^2 - 1}} \right) \right|, \quad (1)$$

where  $\Delta$  is the BCS energy gap. A nonvanishing  $\gamma$  introduces effectively states within the gap region,  $|E| < \Delta$ , as opposed to the ideal BCS DOS obtained with  $\gamma = 0$  resulting in vanishing DOS within the gap. This model reproduces the features observed in our measurements as is shown in Fig. 1(b). We show that, effectively, the Dynes DOS can be produced from the ideal BCS DOS by weak dissipative environment at temperature  $T_{\text{env}} \gtrsim \Delta/k_B$  promoting photon-assisted tunneling. A similar environment model with comparable parameter values has also been introduced by other authors to explain, e.g., observations of excess errors in normal-state electron pumps [23,24] and Andreev reflection dominated charge transport at low bias voltages in NISIN structures [25].

*Theoretical results.*—For inelastic one-electron tunneling, the rates in forward (+) and backward (−) directions through an NIS junction can be written as

$$\Gamma_{\pm} = \frac{1}{e^2 R_T} \int_{-\infty}^{\infty} dE \int_{-\infty}^{\infty} dE' n_S(E') f_N(E \mp eV) \times [1 - f_S(E')] P(E - E'), \quad (2)$$

at bias voltage  $V$ . Here,  $P(E)$  refers to the probability density for the electron to emit energy  $E$  to the environment [13]. The occupations in the normal and superconducting leads are given by the Fermi functions  $f_{N/S}(E) = [e^{E/(k_B T_{N/S})} + 1]^{-1}$ , respectively. In an ideally voltage-biased junction,  $P(E) = \delta(E)$ . The current through the junction at low temperature of the leads,  $T_N, T_S \rightarrow 0$ , is then  $I^0(V) \equiv e(\Gamma_+^0 - \Gamma_-^0) = \frac{1}{eR_T} \int_0^{eV} dE n_S(E)$ . Thus we obtain the well-known expression for the conductance of the junction as

$$dI^0/dV = R_T^{-1} n_S(eV). \quad (3)$$

In view of Eq. (1), the nonzero linear conductance at low bias voltages, typically observed in experiments as shown in Fig. 1(b), suggests that the superconductor has nonvanishing constant density of states within the gap. Within the Dynes model of Eq. (1), the normalized DOS at low energies  $|E| \ll \Delta$  equals  $\gamma$ , the ratio of the conductance at zero bias and that at large bias voltages. Although this approach is correct mathematically, it is hard to justify the presence of subgap states physically.

Here we base our analysis on the pure BCS DOS ( $\gamma = 0$ ) and show that the Dynes model in Eq. (1) is consistent with weakly dissipative environment when Eq. (2) is used to obtain the current  $I(V) = e(\Gamma_+ - \Gamma_-)$ . The effective resistance value  $R = \alpha R_{\text{env}}$  of the environment arises generally from a possibly larger real part of the environment impedance,  $R_{\text{env}}$ , which is suppressed by a factor of  $\alpha$  due to low-temperature filtering; see Fig. 2. With this environment, one obtains the probability density  $P(E)$  in the limit

of small  $R \ll R_Q \equiv \hbar/e^2$  and for energies  $E \ll \hbar(RC)^{-1}$ ,  $k_B T_{\text{env}}$  as a Lorentzian [26]

$$P(E) \simeq \frac{1}{\pi\Delta} \frac{\sigma}{\sigma^2 + (E/\Delta)^2}, \quad (4)$$

where  $\sigma = Rk_B T_{\text{env}}/(R_Q \Delta)$ . As the current of an NIS junction is determined by the values of  $P(E)$  at  $|E| \lesssim \Delta$ , we can apply Eq. (4) when  $k_B T_{\text{env}} \gtrsim \Delta$ ; see Fig. 2 for a numerical demonstration. For a general symmetric  $P(E)$  and  $T_N, T_S \rightarrow 0$ , one obtains from Eq. (2) in analogy with Eq. (3):  $I(V) = \frac{1}{eR_T} \int_0^{eV} dE n_S^{\sigma}(E)$ , and

$$dI/dV = R_T^{-1} n_S^{\sigma}(eV), \quad (5)$$

where the effective DOS is given by the convolution

$$n_S^{\sigma}(E) \equiv \int_{-\infty}^{\infty} dE' n_S(E') P(E - E'). \quad (6)$$

For the weak resistive environment described by Eq. (4), the convolution of a Lorentzian gives

$$n_S^{\sigma}(E) = \left| \Re e \left( \frac{E/\Delta + i\sigma}{\sqrt{(E/\Delta + i\sigma)^2 - 1}} \right) \right|. \quad (7)$$

This expression is identical to the Dynes DOS in Eq. (1) by setting  $\sigma = \gamma$ , with the equivalent inverse lifetime  $e^2 k_B T_{\text{env}} R/\hbar^2$ . The correspondence between the  $P(E)$  theory and the Dynes model, our main theoretical result, is valid for nonzero lead temperatures as well, as we show in the supplementary material [26]. Below, we present numerical and experimental studies verifying our claim.

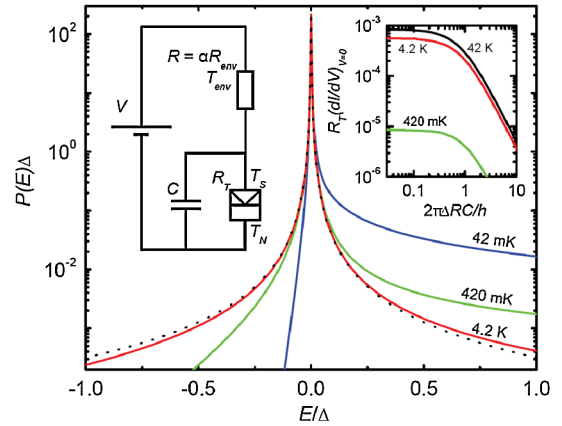


FIG. 2 (color online). The probability density  $P(E)$  calculated for  $\sigma = 10^{-3} = RT_{\text{env}}k_B/(R_Q \Delta)$  and for a few values of the environment temperature  $T_{\text{env}} = 0.042, 0.42,$  and  $4.2$  K. The dotted line is the corresponding Lorentzian limit of Eq. (4). The left inset shows the employed circuit model of an NIS junction (the rectangular symbol at the bottom right) in an RC environment. The right inset shows the calculated zero-bias conductance of the NIS junction as a function of the capacitance  $C$  with the environment corresponding to  $\sigma = 10^{-3}$  and  $T_{\text{env}} = 0.42, 4.2,$  and  $42$  K. We use  $\Delta = 200 \mu\text{eV} \simeq k_B \times 2.3$  K for aluminum.

*Experiments on single junctions.*—The leakage induced by the electromagnetic environment can be decreased by efficient rf filtering of the leads and electromagnetic shielding of the sample. One way to do this without affecting the properties of the junction itself is to increase the capacitance  $C$  across it; see Fig. 2. In this way, one approaches the case of an ideally voltage-biased junction. In Fig. 2, we present the zero-bias conductance of an NIS junction as a function of the shunting capacitance  $C$  based on the full numerical  $P(E)$  calculation. For low  $C$ , the result using Eq. (7) is valid, but for sufficiently high  $C$ , i.e., for  $\Delta RC/\hbar \gtrsim 1$ , the leakage decreases significantly, demonstrating that capacitive shunting is helpful in suppressing the photon-assisted tunneling.

To probe the effect of the capacitive shunting in our experiments, we introduced a ground plane under the junctions. The junctions were made on top of an oxidized silicon wafer, where first a conductive 100-nm-thick Al layer working as the ground plane was sputtered. On top of this, a 400-nm-thick insulating high-quality  $\text{Al}_2\text{O}_3$  film was formed by atomic layer deposition. The junctions were patterned by conventional soft-mask electron beam lithography on top of  $\text{Al}_2\text{O}_3$ . For comparison, junctions were made both with and without the ground plane.

The experiments reported here were performed in a  $^3\text{He}$ - $^4\text{He}$  dilution refrigerator with a base temperature of about 50 mK. All the leads were filtered by using 1.5 m of Thermocoax cable between the 1-K stage and the sample stage at the base temperature. The  $IV$  curves such as the one in Fig. 1(b) are thermally smeared at elevated temperatures, but below 200 mK we observe hardly any temperature dependence. Figure 3 shows the  $IV$  curves measured at the base temperature for one junction on top of a ground plane and for a similar junction without the ground plane, together with numerical results from the  $P(E)$  theory. The capacitive shunting decreases the zero-bias conductance significantly. The shunt capacitance values employed in the  $P(E)$  theory, 10 and 0.3 pF, respectively, match well with the estimates for the experimental values in each case. The sample without a ground plane with  $C = 0.3$  pF is already entering the regime, where the capacitance is too small to play a role. We used an effective environment resistance of  $R = 2 \Omega$  at  $T_{\text{env}} = 4.2$  K, close to the values inferred by Hergenrother *et al.* [25] in the case of incomplete shielding. However, the choice of  $T_{\text{env}}$  is somewhat arbitrary here:  $T_{\text{env}} > 4.2$  K with correspondingly lower  $R$  would yield a slightly improved fit to the data, but  $T_{\text{env}} = 4.2$  K, the temperature of the outer shield, was chosen as a natural surrounding in the measurement setup. Our results with capacitive shunting, on the other hand, correspond to much improved shielding in the language of Ref. [25]. Although the experiments of Ref. [25] are quite different from ours, their situation resembles ours in the sense that photons with a very high frequency of  $\Delta/h \gtrsim 50$  GHz are responsible for tunneling.

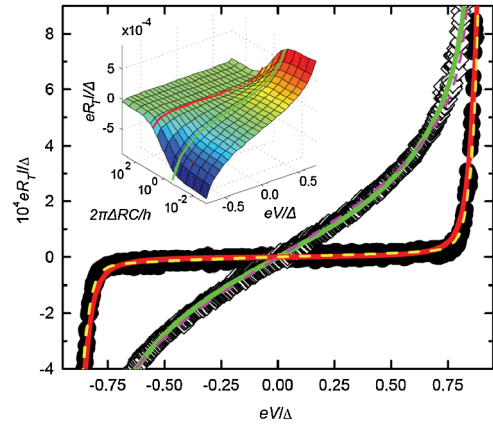


FIG. 3 (color online). Measured  $IV$  curves of an NIS junction with  $R_T = 761$  k $\Omega$  on the ground plane (solid symbols) and of a similar junction with  $R_T = 627$  k $\Omega$  without the ground plane (open symbols). Solid lines present the results of the full  $P(E)$  theory for capacitance  $C = 10$  pF (red line) and  $C = 0.3$  pF (green line). The resistance and the temperature of the environment are set to  $R = 2 \Omega$  and  $T_{\text{env}} = 4.2$  K, respectively, and  $\Delta = 200 \mu\text{eV}$ . The dashed lines correspond to the Dynes model with the parameters yielding the best fit to the data. The normalized zero-bias slope is  $5.3 \times 10^{-4}$  for the green line and  $2.6 \times 10^{-5}$  for the red line. The inset shows  $IV$  curves based on the full  $P(E)$  calculation as functions of the shunt capacitance  $C$ . The red and green lines are reproduced on this graph from the main figure.

*SINIS turnstile.*—As a practical application, we discuss the SINIS turnstile, which is a hybrid single-electron transistor (SET) and a strong candidate for realizing the unit ampere in quantum metrology [4,27–30]. In the previous experimental studies [4,27,29], its accuracy was limited by the subgap leakage. Here we test the influence of the ground plane on the flatness of the current plateaus at multiples of  $ef$ , where  $f$  is the operating frequency. The ground plane had a 20- $\mu\text{m}$ -wide gap under the SET to reduce the stray capacitance to the rf gate. The ground plane layer was covered by a 300-nm-thick insulating layer of spin-on glass, on top of which the rf gate and dc leads were evaporated. Another 300-nm spin-on glass layer was used to cover the rf gate, and the SET was fabricated on top of this layer. The device is shown in Fig. 4(a). This sample geometry is designed for parallel pumping [30], but here we concentrate on a single device.

Figure 4(b) shows that in this case, the introduction of the ground plane reduces the subgap leakage by roughly 2 orders of magnitude as opposed to a typical turnstile without the ground plane (the latter data from Ref. [29]). In the turnstile operation, the current was recorded as a function of the amplitude of the sinusoidal rf drive,  $A_g$ , at several bias voltages. In Fig. 4(c), we show the quantized current plateau at  $f = 10$  MHz, and the averaged current on this plateau is given in Fig. 4(d) as a function of the bias voltage. The differential conductance at the plateau divided

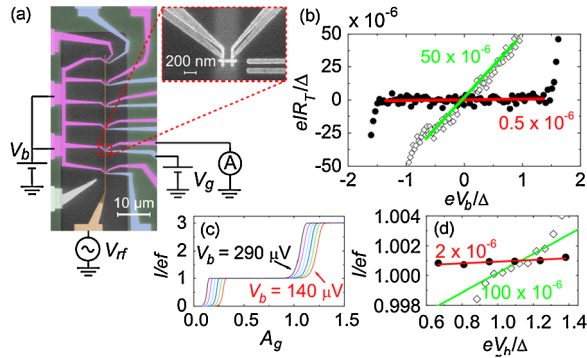


FIG. 4 (color online). (a) Scanning electron micrographs of the SINIS turnstiles. (b) Subgap  $IV$  curves of the measured transistors in the gate-open state (charge degeneracy). The slope of the linear fit corresponds to the leakage of  $0.5 \times 10^{-6}$  for the sample with the ground plane (filled circles) and  $50 \times 10^{-6}$  for the sample without the ground plane (open diamonds) in units of the asymptotic conductance of each SET. (c) Current through the turnstile on the ground plane as a function of the amplitude of the applied sinusoidal gate drive at  $f = 10$  MHz. The gate offset was set to the charge degeneracy point, and the bias voltage was varied uniformly between  $V_b = 140$  and  $290 \mu\text{V}$ . (d) Current at the first plateau as a function of  $V_b$  obtained from data similar to those in (c) (filled circles) showing leakage of  $2 \times 10^{-6}$  and for the sample without the ground plane (open diamonds) with leakage of  $100 \times 10^{-6}$  and a reduced step width.

by the asymptotic conductance of the SET is  $2 \times 10^{-6}$ . This result is much improved over those of the earlier measurements [4,27,28] and that of the reference sample without the ground plane.

In conclusion, we have shown analytically that the Dynes density of states can originate from the influence of the electromagnetic environment of a tunnel junction, and it is not necessarily a property of the superconductor itself. Our experiments support this interpretation: We were able to reduce the leakage of an NIS junction by an order of magnitude by local capacitive filtering. We stress that capacitive shunting does not necessarily suppress the subgap leakage of an NIS junction, if the leakage is caused by the poor quality of the junction or by true states within the gap due to, e.g., the inverse proximity effect [3]. Protecting the junctions against photon-assisted tunneling improves the performance of, e.g., single-electron pumps. Contrary to the resistive environment aiming at the same purpose [28], capacitive shunting does not limit the tunneling rates.

We thank D. Averin, P. Delsing, M. Gustafsson, H. Im, S. Lotkhov, A. Manninen, M. Paalanen, and V. Shumeiko for discussions and M. Meschke, J. Peltonen, and I. Iisakka for technical support. This work has been supported by Technology Industries of Finland Centennial Foundation,

the Academy of Finland, Emil Aaltonen Foundation, the Funding Program for World-Leading Innovative R&D on Science and Technology (FIRST), CREST-JST, MEXT kakenhi “Quantum Cybernetics,” and the European Community’s FP7 Programme under Grant Agreements No. 228464 (MICROKELVIN, Capacities Specific Programme), No. 217257 (EURAMET joint research project REUNIAM), and No. 218783 (SCOPE).

\*On leave from P.N. Lebedev Physical Institute, Moscow 119991, Russia.

- [1] Ya. M. Blanter and M. Büttiker, *Phys. Rep.* **336**, 1 (2000).
- [2] *Quantum Computing with Superconducting Qubits*, Quantum Inf. Process. Vol. 8 (Springer, New York, 2009), pp. 51–281.
- [3] F. Giazotto *et al.*, *Rev. Mod. Phys.* **78**, 217 (2006).
- [4] J. P. Pekola *et al.*, *Nature Phys.* **4**, 120 (2008).
- [5] J. Bardeen, L. N. Cooper, and J. R. Schrieffer, *Phys. Rev.* **108**, 1175 (1957).
- [6] G. C. O’Neill *et al.*, *J. Low Temp. Phys.* **151**, 70 (2008).
- [7] S. Rajauria *et al.*, *J. Low Temp. Phys.* **153**, 325 (2008).
- [8] P. Koppinen *et al.*, *J. Low Temp. Phys.* **154**, 179 (2009).
- [9] H. Jung *et al.*, *Phys. Rev. B* **80**, 125413 (2009).
- [10] D. C. Ralph *et al.*, *Phys. Rev. Lett.* **74**, 3241 (1995).
- [11] R. C. Dynes *et al.*, *Phys. Rev. Lett.* **41**, 1509 (1978).
- [12] R. C. Dynes *et al.*, *Phys. Rev. Lett.* **53**, 2437 (1984).
- [13] G. L. Ingold and Yu. V. Nazarov, in *Single Charge Tunneling*, edited by H. Grabert and M. H. Devoret, NATO ASI Series B, Vol. 294 (Plenum Press, New York, 1992), pp. 21–107.
- [14] D. V. Averin and Yu. V. Nazarov, *Phys. Rev. Lett.* **65**, 2446 (1990).
- [15] A. F. Andreev, *Zh. Eksp. Teor. Fiz.* **46**, 1823 (1964) [*Sov. Phys. JETP* **19**, 1228 (1964)].
- [16] G. E. Blonder *et al.*, *Phys. Rev. B* **25**, 4515 (1982).
- [17] T. M. Eiles *et al.*, *Phys. Rev. Lett.* **70**, 1862 (1993).
- [18] H. Pothier *et al.*, *Phys. Rev. Lett.* **73**, 2488 (1994).
- [19] J. M. Hergenrother *et al.*, *Phys. Rev. Lett.* **72**, 1742 (1994).
- [20] S. Rajauria *et al.*, *Phys. Rev. Lett.* **100**, 207002 (2008).
- [21] M. Nahum and J. M. Martinis, *Appl. Phys. Lett.* **63**, 3075 (1993).
- [22] J. M. Martinis *et al.*, *Phys. Rev. Lett.* **103**, 097002 (2009).
- [23] M. W. Keller *et al.*, *Phys. Rev. Lett.* **80**, 4530 (1998).
- [24] J. M. Martinis and M. Nahum, *Phys. Rev. B* **48**, 18316 (1993).
- [25] J. M. Hergenrother *et al.*, *Phys. Rev. B* **51**, 9407 (1995).
- [26] See supplementary material at <http://link.aps.org/supplemental/10.1103/PhysRevLett.105.026803> for derivation.
- [27] A. Kemppinen *et al.*, *Eur. Phys. J. Special Topics* **172**, 311 (2009).
- [28] S. V. Lotkhov *et al.*, *Appl. Phys. Lett.* **95**, 112507 (2009).
- [29] A. Kemppinen *et al.*, *Appl. Phys. Lett.* **94**, 172108 (2009).
- [30] V. F. Maisi *et al.*, *New J. Phys.* **11**, 113057 (2009).